Dynamic analysis and performance of a Repoint track switch

Y. Bezin[a], M.L. Sarmiento-Carnevali[b*], M.Sh. Sichani[a], S. Neves[a], D. Kostovasilis[a],
S.D. Bemment[b], T.J. Harrison[b], C.P. Ward[b] and R. Dixon[c]

[a]*Institute of Railway Research, School of Computing and Engineering, University of
Huddersfield, Huddersfield, West Yorkshire, United Kingdom;*
[b]*Wolfson School of Mechanical, Electrical and Manufacturing Engineering, Loughborough
University, Loughborough, Leicestershire, United Kingdom;*
[c]*School of Engineering, University of Birmingham, Edgbaston, Birmingham, United Kingdom*

(*v4.0 released November 2018*)

Repoint is an alternative concept for the design of track switches developed at Lough-
borough University. The concept, based around a stub switch, offers several improvements
over current designs. Through a novel locking arrangement, it allows parallel, multi-channel
actuation and passive locking functions, providing a high degree of fault tolerance. The aim
of the work presented in this paper is to evaluate the dynamic interaction forces due to the
passage of rolling stock over the switch and, particularly, the area of the stub rail ends, in
comparison to a conventional switch. Specific behaviour and load transfer conditions from
one rail to the other at the joint are analysed, as well as long term wear conditions of the
rails. These evaluations are undertaken by means of multi-body dynamic simulations, lead-
ing to design refinement of the stub rail ends and the identification of further research and
development requirements in their design.

Keywords: track switch; wheel-rail contact; vehicle-track interaction; multi-body physics;
kinematics; vehicle dynamics

1. Introduction

Railway track switching provides flexibility to a rail network, allowing vehicles to transfer
between many different routes. Existing track switch systems are the result of the evo-
lution of a single design solution patented by Charles Fox in 1836 [1]. However, current
approaches do not have major functional changes in comparison with the original design.
The Repoint switching concept [2–4] challenges this design paradigm. Multiple potential
benefits are possible using this approach: from maintenance; to operational methods;
with the paper focusing on the dynamic benefits to the vehicles traversing the switch
and also the impact on the track switch panel.

Figure 1 shows a classic track switch layout with sleepers and bearers omitted for
clarity. A pair of longitudinally extending switch rails (6) are free to bend or pivot
beyond a given point towards the heel and slide upon supporting plates or chairs, between
two fixed stock or running rails (7). Actuation power and transmission can variously
be provided by humans and mechanical lever arrangements(1). A mechanical linkage

---

*Corresponding author. Email: m.l.sarmiento-carnevali@lboro.ac.uk

from the power source links the two switch rails via stretcher bars (2,5), to open one rail and close the other, either synchronously or sequentially. Mainline switches which carry passenger traffic tend to feature an active locking arrangement which prevents the switch rails moving uncommanded or when incorrectly commanded, for instance under the wheels of a passing train. Standard designs of switches of different lengths and crossing (8) angles exist to satisfy different turnout speeds: longer switches generally being more complex and expensive, but capable of handling traffic turning out at much higher speeds.
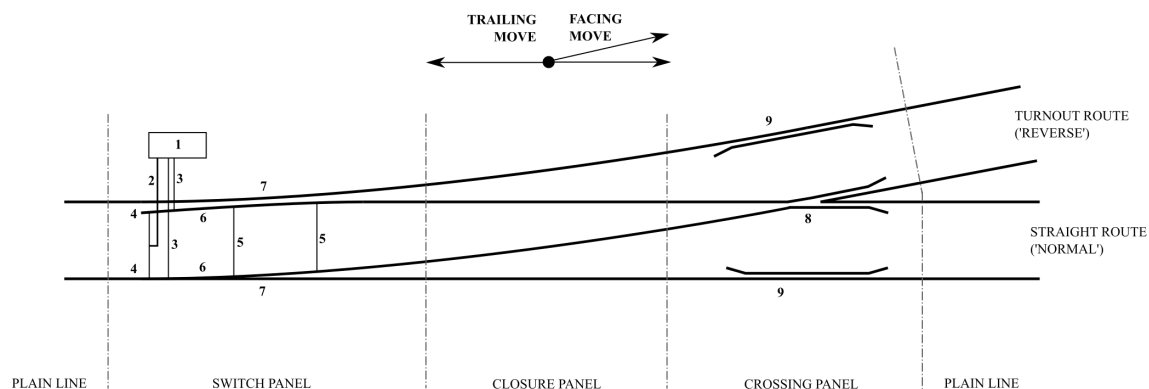
Figure 1. Traditional switch layout, with sleepers/bearers omitted for clarity. Numbered elements are: (1) lineside type electro-mechanical actuator featuring integral lock and detection (actuation/locking mechanism), (2) drive rod and drive stretcher (actuation mechanism), (3) detection rods (detection mechanism), (4) switch rail toes, (5) stretcher bars (actuation mechanism), (6) switch rails, (7) stock rails, (8) common crossing (of given angle) and (9) check rails.

Current track switches are not designed with fault tolerance in mind and contain multiple potential single point failures (stretcher bars, actuators, locking mechanisms, etc.); failure of any one of these can prevent the use of extensive sections of the network. It is for this reason that rail network performance is negatively affected by switch failures to a greater degree than any other asset [2, 3, 5]. Therefore, improvement of railway switches and crossings is an active field of study due to the importance of such assets. Comprehensive analyses of rail vehicles passing through different turnout designs have been performed [6] and often including analysis of damage on rail components [7–9]. Methods for the optimisation of switch rail profile and layout geometry are presented in [10, 11]. Methods for the optimisation of switch support are presented in [11–13]. Wheel-rail impact analysis have also been performed on various crossings [14–17] using similar methodologies. Essentially, these works resulted in small modifications of a traditional track switch and none considered the issue of redundancy and fault tolerance, or the basic track arrangement.

The Repoint concept is intended to reduce the effect of switch failures by introducing redundant actuation and passive locking; it is designed to be a fail-safe solution with 'graceful' degradation of actuation, since an individual actuator can fail but the overall system will still be capable of setting routes [2, 3]. Additionally, a new track layout is envisaged with 'full section' rails throughout, which would eliminate the majority of the issues of the transfer from stock to switch rail (and in the inverse) with the large and rapid changes in contact angle and rolling radii this entails. Figure 2 shows the main Repoint switch elements: (1) in-bearer type electro-mechanical actuators, (2) bearer featuring integral passive locking elements, (3) bendable, full-section switch rails, (4) interlocking rail ends, (5) lineside processing and condition monitoring cabinet, (6) power, position

and monitoring signal cables, (7) stationary point of curve, (8) common crossings (of given angles) and (9) check rails.
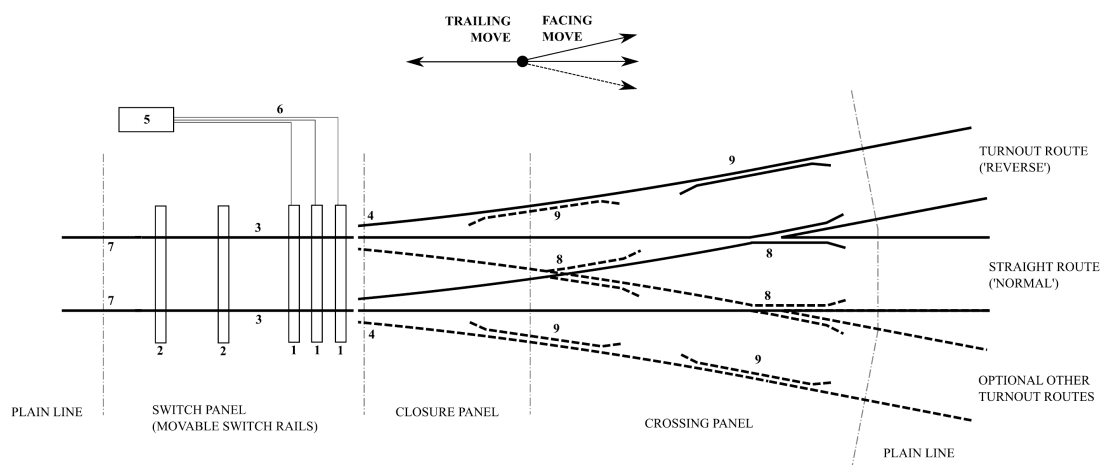

Figure 2.   Repoint stub switch general arrangement with electro-mechanical in-bearer type actuators, with most sleepers/bearers omitted for clarity. Switch panel features rail moveable elements [2, 3].

Figure 3 shows the interlocking rail ends that are required for alignment of the full section rails. On the rail ends, a chamfer in the horizontal plane locates the rails laterally, meaning the moveable rails require lifting to disengage this chamfer before they can be moved horizontally. The main design change from a conventional switch actuation mechanism is that the Repoint actuators operate the switch rails through a two-dimensional arc, lifting them out of register before traversing them and then lowering them in the opposite register (see Figure 4). The concept allows for some longitudinal movement of the rails in the same way an expansion switch operates, thus accounting for thermal changes. The chamfer in the vertical plane gives a smooth transfer of load from one rail to the other and reduces the chance of debris fouling the interface.

The support mechanism below this critical joint is not illustrated. If unsupported there is the possibility of the joint flexing with the passage of a vehicle, altering the contact area dramatically. Though not explicitly shown, the assumption is that additional vertical support will be used. This would be similar to the 'Baulk road' concept of longitudinal rail support used initially by Brunel, now more commonly referred to as 'ladder track' [18]. The modelling in this paper assumes a constant support stiffness model underneath the rails and therefore complies with the previous assumption.

This paper focuses on how the Repoint system removes the need for a classical switch/stock rail assembly, which is expected to improve the dynamic forces and vehicle behaviour in comparison to a conventional switch panel. The following sections present the result of an exhaustive analysis of the dynamic interaction forces due to the passage of rolling stock over the various routes of a Repoint Switch, and compares these dynamic results to traditional UK switch designs. Results were generated through the multibody dynamics simulation software VI-Rail [19]. The paper is organised as follows: section 2 presents a comprehensive analysis of wheel-rail mechanical interface dynamic forces on Repoint in comparison with a traditional UK CV switch geometry; section 3 introduces initial results on wear analysis for the Repoint concept; and finally section 4 contains conclusions and scope for future work.
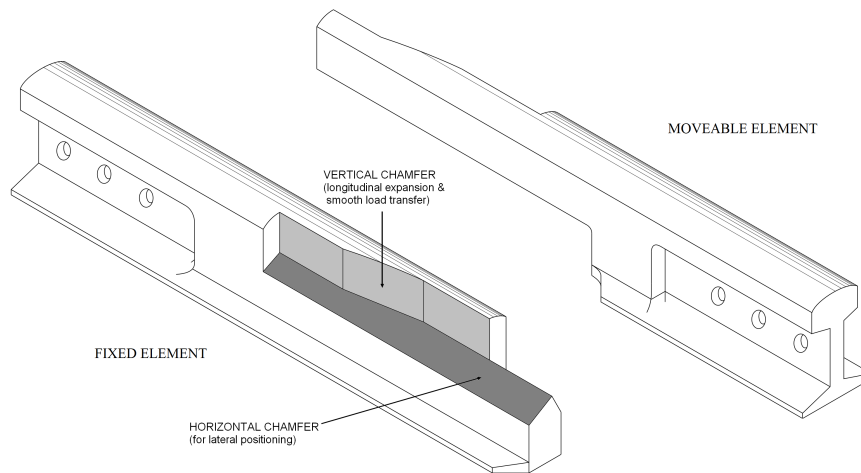
Figure 3. Interlocking rail ends (together represent the Repoint Joint). Moveable elements lie on in-bearer type actuators in the switch panel [2, 3].
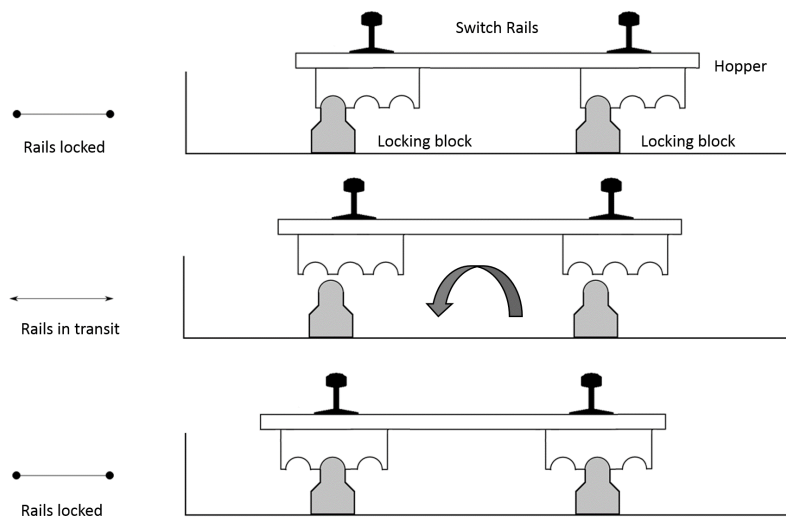

Figure 4. Cross section through an actuator bearer showing switch rails movement.

2. Dynamic wheel-rail force comparative analysis

In order to quantify the dynamic performance improvement of a Repoint system, direct comparisons are drawn with an existing standard switch design, the UK CV type switch. In track switching context, C stands for the category (slow turnout speed of 40 kph with 245 m radius) and V stands for vertical rail installation. This is a short switch geometry, approximately 25 m in length between the toe and the crossing nose, with a turnout radius of 245 m and a crossing angle of 1 in 9.25. The limit speed in the turnout direction is 40 kph, which is the speed used for all the simulations in this work for the diverging direction. This type of turnout is widely representative of UK track and, despite its short length and wide crossing angle, it can be found on intercity routes

with 200kph speed in the through direction. It is also the type of crossing presenting the highest number of faults and the most severe wheel-rail interaction due to the tight turnout radius. Therefore, this makes it an ideal candidate to be compared with Repoint, both in the switching functionality and possible improvements in running performance.

The reference rail profile used for this switch corresponds to CEN56 rails [20], which are vertically installed in the CEN56 CV switch for ease of commissioning and fixing. However, in the Repoint concept there is no constraint of having to use vertical rails, thus a UK generic inclination of 1 in 20 can be used throughout, to maintain plain line conditions in terms of contact both in the straight through and diverging routes.

In Figure 5, a plan view track geometry layout of the turnout is shown, together with specifics of the track curvature as a function of distance along the switch panel. Dashed vertical lines indicate the longitudinal position of the Repoint Joint (labelled RePt.Jt), switch toe, heel and crossing nose (labelled Xg). Four geometries are used in this comparative analysis:

(A) Standard CEN56 CV turnout switch (British Standard 13674-2, 2006) with vertical rails (thick red line).
(B) Adjusted idealised geometry. This is a normal plain rail with 2/3rd reduced curvature (increased radius) and increased length of transition and curve to maintain identical crossing position, where straight rail meets the diverging one. Although this leads to a shallower crossing angle, it is added for reference to see how steering conditions can be improved with an ideal running rail and a longer foot print area for the complete turnout (light orange line).
(C) Repoint switch geometry; excluding the details of the stub joints and the chord offset explained in Figure 6 (light grey thick line partly covered by D in Figure 5).
(D) Full Repoint switch (thick black line).

Note that the straight chord offset at the rail stub ends joint is a necessary geometry feature to allow for the manufacturing and good functioning of the stub joints inter-connection. At this location, a deviation from ideal curvature is necessary, which has a certain impact on the wheel-rail guidance as seen later. The chord offset (or versine) is calculated over a 3 m chord length using Hallade's method [21, 22] such that:

$$v_{offset} \approx \frac{L^2}{8R} = 4.58mm, \tag{1}$$

where L indicates chord length and R is radius of curvature.

Repoint does not rely on the machining of switch rails as does the reference CV switch, therefore, the earlier geometry (length and transition) can be extended and is mainly dictated by the requirement for a certain number of active (actuated) and passive bearers. While for the CV switch the track curvature suddenly appears ≈1.8 m ahead of the toe (situated at 30 m in bottom Figure 5), in Repoint it can start earlier x=23.8 m and build up over 9 m at x=32.8 m. Beyond this point, both designs have the same x-y plan track geometry, except for the chord offset, added in the simulation as a outer and inner rail irregularity to ensure straightness of the joint.

Note that in cases where Repoint might be compared to longer switch geometries, either tangential or non-intersecting with clothoid, the advantages gained would be reduced in terms of layout geometry; and the gains will mainly concern the elimination of the switch and stock rail discontinuity in terms of wheel guidance. The rail inclination is also often maintained in practice on longer switches.
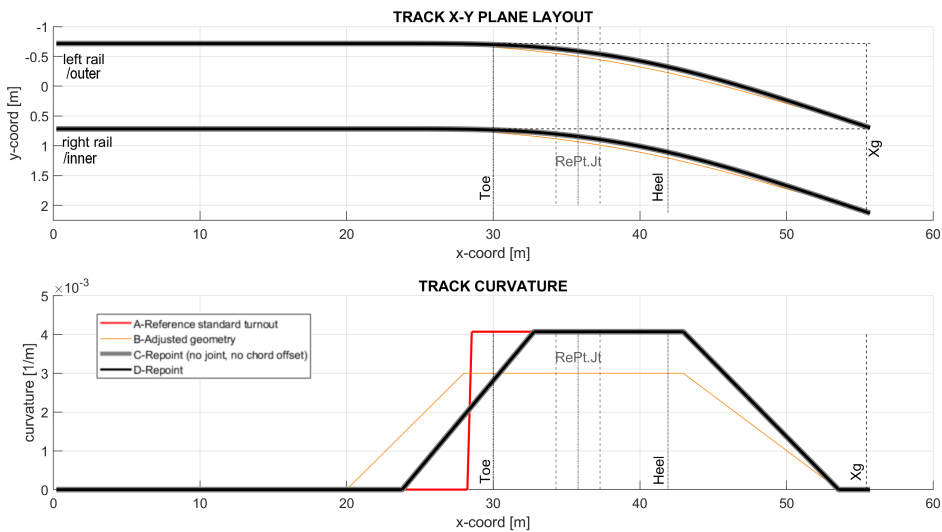
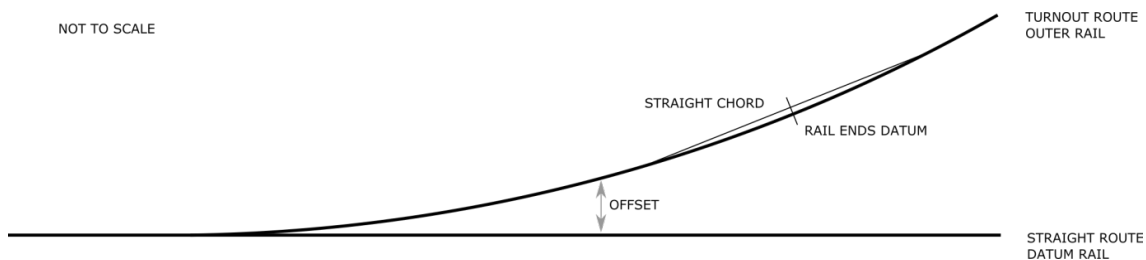Figure 5. Track layout geometry (top) and curvature (bottom).

Figure 6. Sketch (not to scale) of straight chord offset at stub rail ends point.

In terms of the Repoint joint (rail ends) development, it is necessary to ensure smooth wheel-rail contact running behaviour. To do so a starting design was inspired from expansion joints [23–25] and applied here to a situation where harsh curving conditions are expected. Figure 7 shows the 3D geometry used as input to generate the series of 2D cross sections required for the multi-body simulation software and highlights a few areas of improvement of the joint, discussed alongside the initial results.

All simulations are carried out using the standard flexible co-running track model in VI-Rail [26], assuming constant properties along the track. Although in practice there are inherent support stiffness variations along a turnout, the limitations of this approach are deemed reasonable when looking at the general vehicle dynamics and wheel-rail contact; and also reinforced by the assumptions that the support below the joint will be continuous as discussed previously in section 1. Further design work of the support structure would require using more detailed FE analysis methods outside the scope of this paper. The vehicle model represents a UK Diesel Multiple Unit class 170 (DMU170) - properties are shown in the Appendix. Results are focused on the leading bogie and carbody outputs only. Note that considering a range of primary/secondary yaw stiffness, and wheel profiles, would influence variability in the results obtained in the simulations. The trailing bogie is assumed to behave in a similar or better manner with respect to the leading one, due to the fact that the leading bogie steers the whole vehicle into the curve by the time the rear one enters the switch. In all time domain analysis figures hereafter,
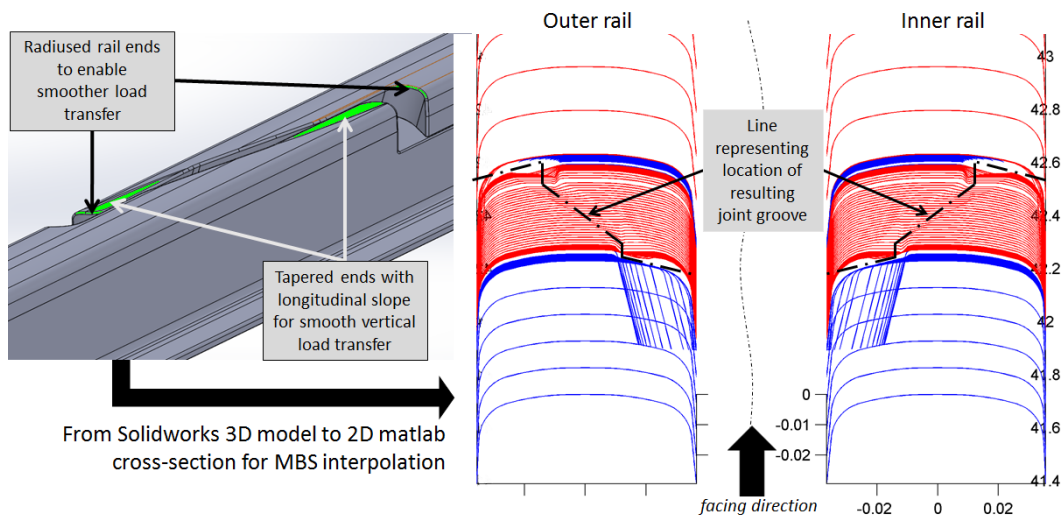
Figure 7. 3D geometry for stub rail end joint and individual cross section definition for simulation. Blue and red colors indicate different longitudinal sections of the joint.

the following are added for comprehension:

- Leading axle of leading bogie is shown as a solid line.
- Trailing axle of leading bogie is shown as a dashed line.
- With the exception of section 2.1 (through direction), travelling route is diverging, right hand side turnout.
- Travelling direction is always facing as indicated.
- Outer rail is always on the upper figure and inner rail on the lower figure. They correspond to the outer and inner rails respectively (right hand side turnout).
- Longitudinal position of reference CV switch toe, heel and crossing nose (Xg) are indicated with vertical dashed, dotted or semi-dashed lines. Note that the change in rail cross section in the crossing area is ignored in these simulations as Repoint is purely focused on the switch panel improvement and no changes are expected there.
- The longitudinal position of the Repoint joint (RePt.Jt) and start/end of the chord offset are indicated with grey vertical semi-dashed and dashed lines respectively.

2.1. *Straight through direction analysis*

In a first instance the behaviour of the Repoint switch is compared to the UK CV switch in the straight through direction at speeds ranging from 40 kph to 200 kph. In figure 8 the lateral contact forces are presented. Dynamic transient forces in the order of +3 to -12 kN are observed for the reference case simply due to the disturbance of the switch-stock rail rolling contact behaviour. On the other hand Repoint shows nearly undisturbed track force behaviour and represent a near ideal situation.

Figure 9 shows the vertical force on the rail with around 25% increased dynamic component occurring in the area of stock to switch rail contact change. The presence of the Repoint joint also leads to a dynamics increase up to 33%, however it is a lot more transient in nature (very short duration) and relates to the movement of the contact point on the upper chamfer edge of the moveable part (see Figure 7, outer rail move from blue sections to red sections).

Figure 10 shows the equivalent Hertzian contact pressure. The initial condition shows
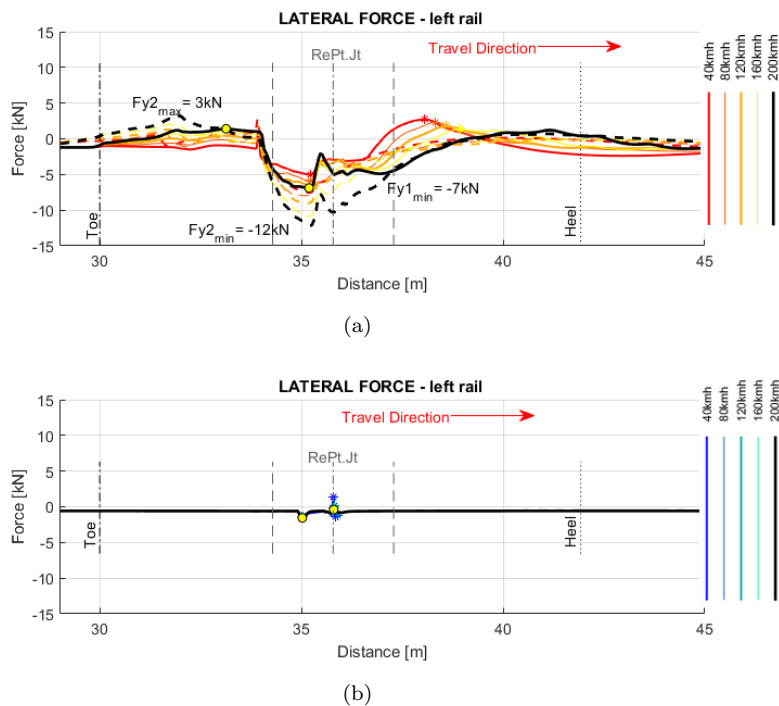
(a)

(b)

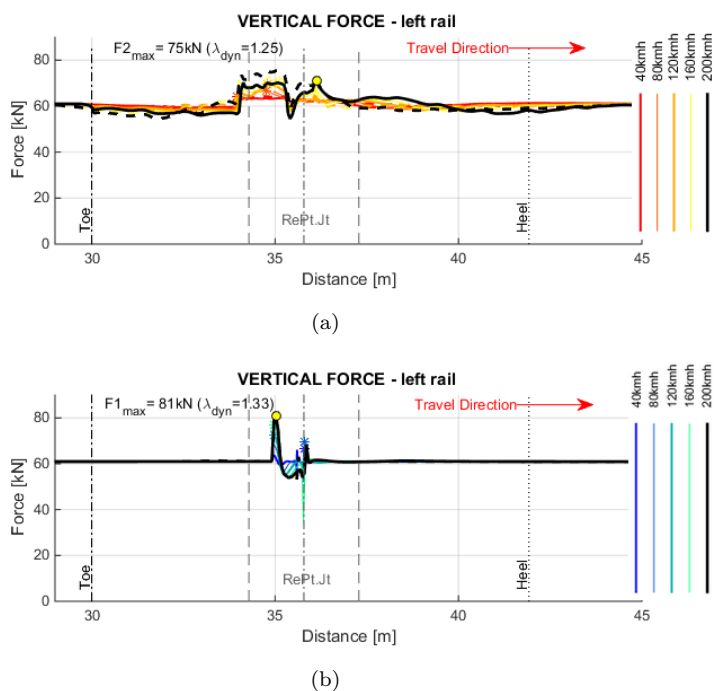Figure 8. Lateral guiding forces on the outer rail for CV (a) and Repoint (b).

(a)

(b)

Figure 9. Vertical force on the outer rail for CV (a) and Repoint (b).

a difference of 750 MPa and 1500 MPa for Repoint and CV respectively. This difference is purely attributed to the vertical rail for CV contacting nearer the gauge corner where the radius is smaller than on the crown of the rail. Additionally, transient high pressure

increase is visible in the area of the stock-switch rail assembly. Repoint on the other hand shows a very steady and low contact pressure throughout, with the exception of a very local and short transient in the area of the joint. This is explained further in the following sections looking at diverging conditions.
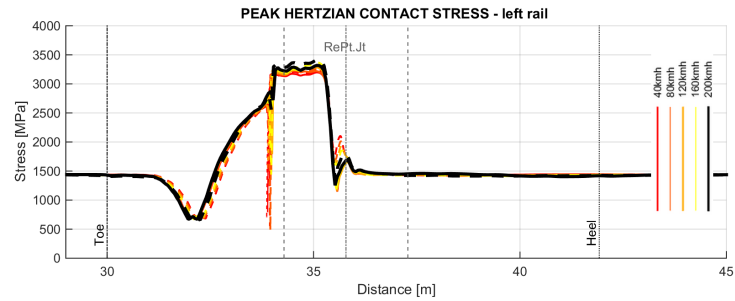

(a)
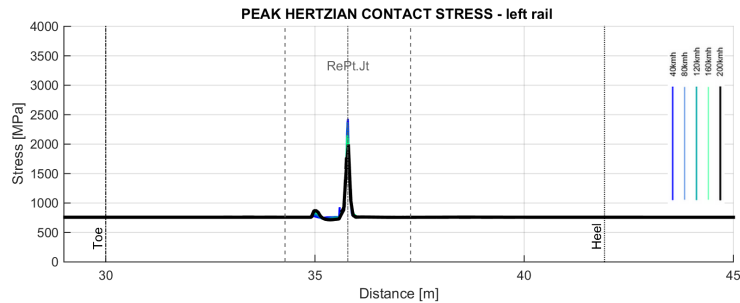
(b)

Figure 10. Peak equivalent Hertzian contact stress for CV (a) and Repoint (b).

Figure 11 shows the lateral acceleration above front bogie pivot generated from the straight through running. Disturbances result from car body lateral reaction under the action of the wheel rolling through the switch-stock rail assembly. While disturbances are small for UK CV (+/-5% of gravitational acceleration), Repoint shows a virtually stable response. Bottom plot y-axis scale is much smaller in comparison. In the through direction the Repoint switch effects would not be felt by a passenger and can therefore offer benefits at high and very high speed.
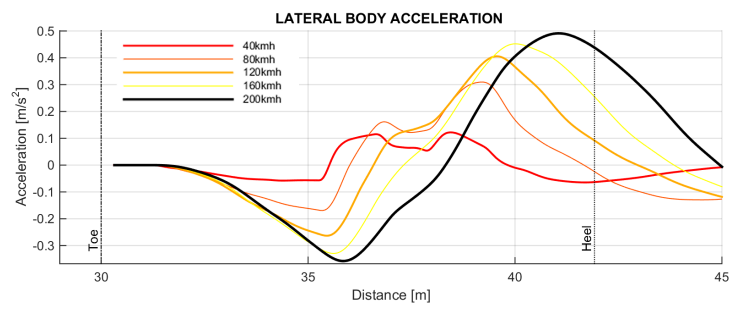
(a)
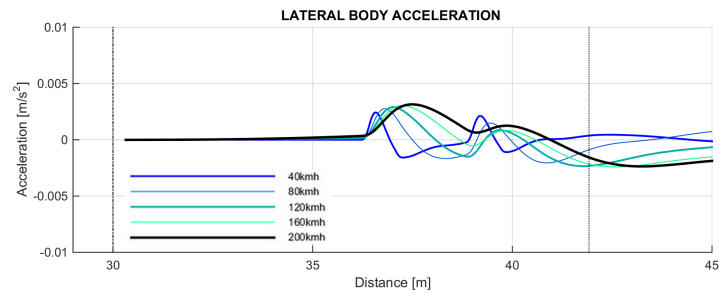
(b)

Figure 11.   Car body lateral acceleration above front bogie pivot for CV (a) and Repoint (a and b y-axis scale is different).

2.2. *Diverging direction analysis: track lateral dynamics*

Figure 12 presents simulation results of the lateral (Fy) contact forces on each wheel. The leading wheelset generates the majority of the steering force, with the outer wheel/rail experiencing larger force than the inner wheel/rail due to a large lateral offset (Fig. 14), and flange contact causing a large contact angle change. The reference CEN56 CV force profile is characterised by sharp rise in lateral force about 1 m after the switch toe, accompanied by dynamic force disturbance due to change in contact from stock to switch rail. This is a typical behaviour in conventional S&C often leading to associated local geometry degradation affecting the safe and reliable operation of Point Operating Equipment, as well as generating incidental costs in managing wear and rolling contact fatigue (RCF) of the stock and switch rails.

The Repoint switch on the other hand shows a slower and more gradual build-up of lateral forces starting at the toe position, eventually rising to the equivalent quasi-static equilibrium forces once in the full switch curve radius. Further dynamic force disturbances are then observed as the leading axle is forced to steer through the chord direction. This is indicated in the area between the vertical dashed lines of the chord length, identified within the text (RePt.Jt). There is a slight rise of steering force before the joint as rails effectively cut through the chord direction, then a decrease and eventually a return to normal quasi-static conditions. This effect is less pronounced on the inner rail, seeing lower steering forces with contact on the crown of the rail.

Additionally, on the outer rail, the joint (RePt.Jt) causes another very short transient of higher magnitude with a sudden drop of lateral force and then a reciprocally high value. This is due to the local transition of contact from the moveable element to the fixed element of the joint, while lateral flange contact is sustained and the expansion gap suddenly appears before the wheel. The wheel then travels further against the rail until it makes contact with the end of the fixed element.

In Figure 12 the idealised switch curve shows slightly improved quasi-static curving conditions on the outer rail compared to both Repoint and reference CV switch, associated with a reduced angle of attack (Figure 14 bottom).

Figure 7 shows the 3D geometry and the 2D cross sections used for simulation. Assuming the wheel is in flange contact on the outer rail, under the action of lateral steering forces, it will traverse the transversal groove in its path when exiting the joint. A quick 3D analysis of the input geometry shows that contact in a 40mm nominal length joint gap would lead to split contact between the end of the movable part and the fixed gauge corner, as illustrated in Figure 13. In this figure a) represents the last contact on the end of the movable part, b) the split contact between both parts assuming a further lateral offset of the wheel of 1mm and c) the full contact on the fixed part. The penetration area obtained from the 3D CAD software under those conditions is highlighted as a light colored yellow patch and is for illustration only, and not based on any contact theory. In this study, the authors are bound by current multi-body simulation capabilities and by the assumption that all contact is calculated at a given longitudinal position using 2D cross sections of wheel and rail. The wheel angle of attack is taken into account by recalculating its shape through an orthogonal projection on the relevant cross sectional plane, however, there is no consideration for longitudinal offset of the contact points. Figure 13 case b) shows that any lateral offset within the groove would be limited (here 1mm for b compared to a and c), and reveals that the local simulated 2mm increment in lateral displacement of the wheelset and associated high transient load are more than likely over-predicted in this paper. However, it is out of the scope of this work to develop a full 3D contact model applicable to multi-body simulation. Nonetheless, the contact of
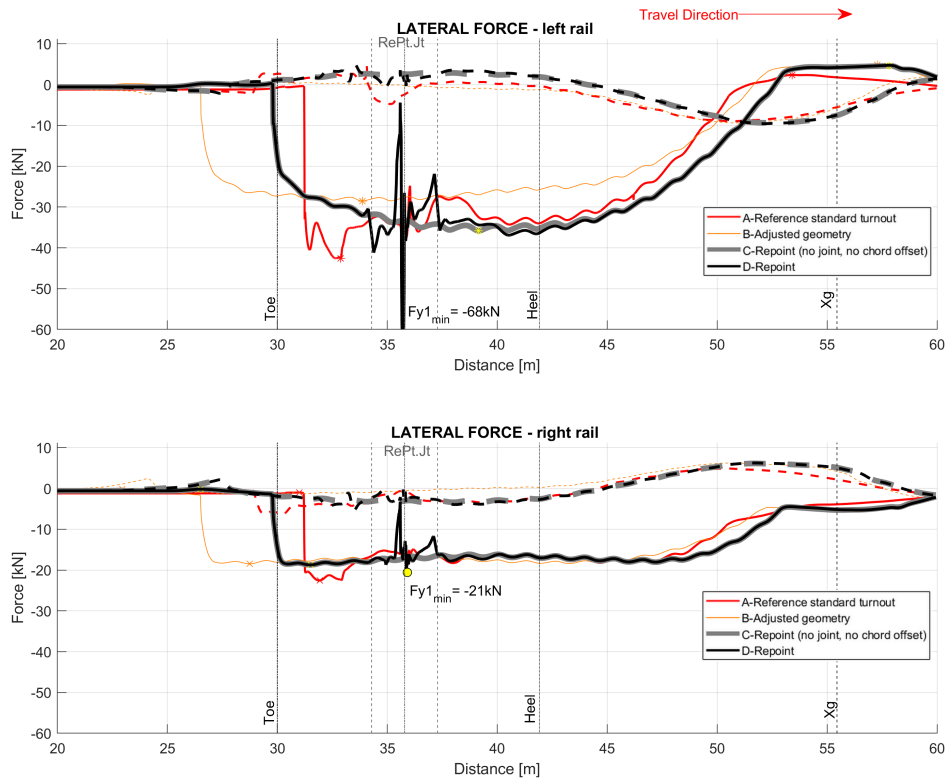
Figure 12. Lateral guiding forces on the wheels (negative means gauge spreading forces on rails). Solid lines (–) for leading axle and dashed lines (- -) for trailing axle.

the wheel on the low rail, or on through route, would occur on the top of the crowned rail and would transit more smoothly from one jointed rail to the other as designed. Despite its limitations, the current modelling approach did help to improve the design of the stub ends thanks to earlier simulated versions of the joint, leading to the addition of tampered ends (horizontal slopes) and radiused ends as indicated in Figure 7 (left), to enable smoother load transfers. The present work highlights likely issues with the current joint design requiring further thoughts and improvements to prevent any transient behaviour, which can lead to undesired damage of both rails material and track support quality in this area.
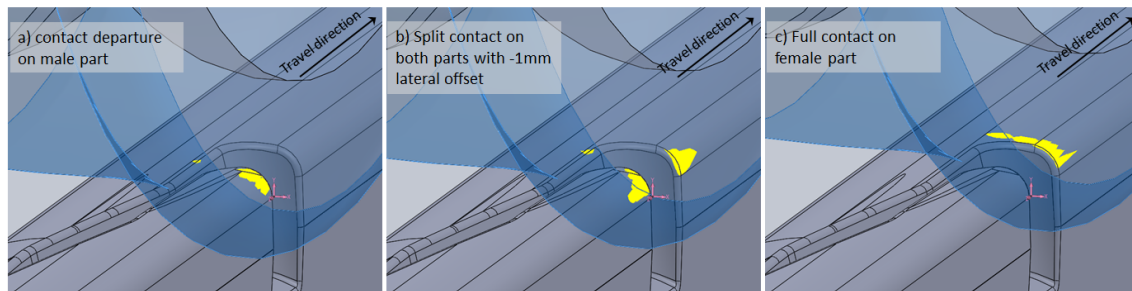

Figure 13. 3D illustration of the likely contact jump in the Repoint joint groove area assuming flange contact and 10mrad angle of attack and a 40mm gap.

Figure 14 clearly shows the large lateral offset of the leading axle from the toe onwards, also confirming this effect is anticipated and more progressive for the Repoint design. This more gradual change in wheel behaviour is observable from the leading axle angle of attack, steadily increasing towards the heel. Some local change of angle of attack is also visible in the area of the joint chord offset, which directly translates to the lateral force disturbance described previously. This effect will also be discussed with respect to contact wear in the following section. On the top plot in Figure 14, the local lateral movement of the axle is seen with an added 2 to 2.5 mm lateral displacement over a very short duration, most likely exaggerated here as discussed above.
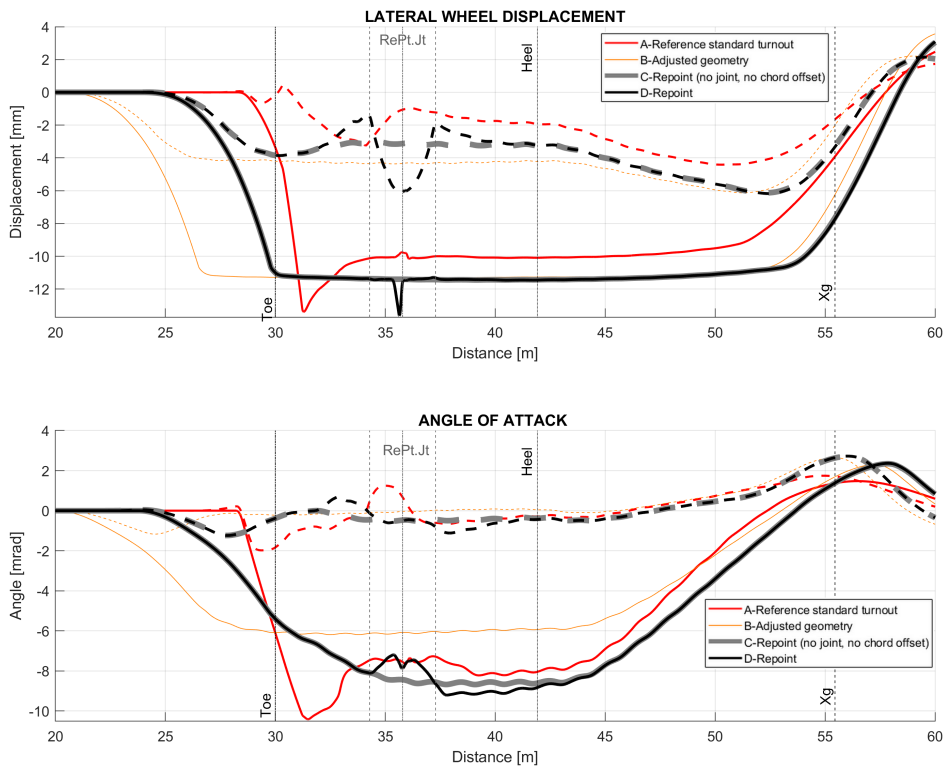
Figure 14.   Axle lateral displacement and angle of attack. Solid lines (–) for leading axle and dashed lines (- -) for trailing axle.

2.3.   *Diverging direction analysis: vertical dynamics*

Figure 15 shows simulation results of the vertical forces. The Repoint switch demonstrates a slightly smoother transition in load up to the Repoint joint. However, both designs show high transient effects either under the switch-stock rail assembly or the Repoint joint, and overall dynamic amplification factors of around +/- 1.35, including centrifugal load imbalance.
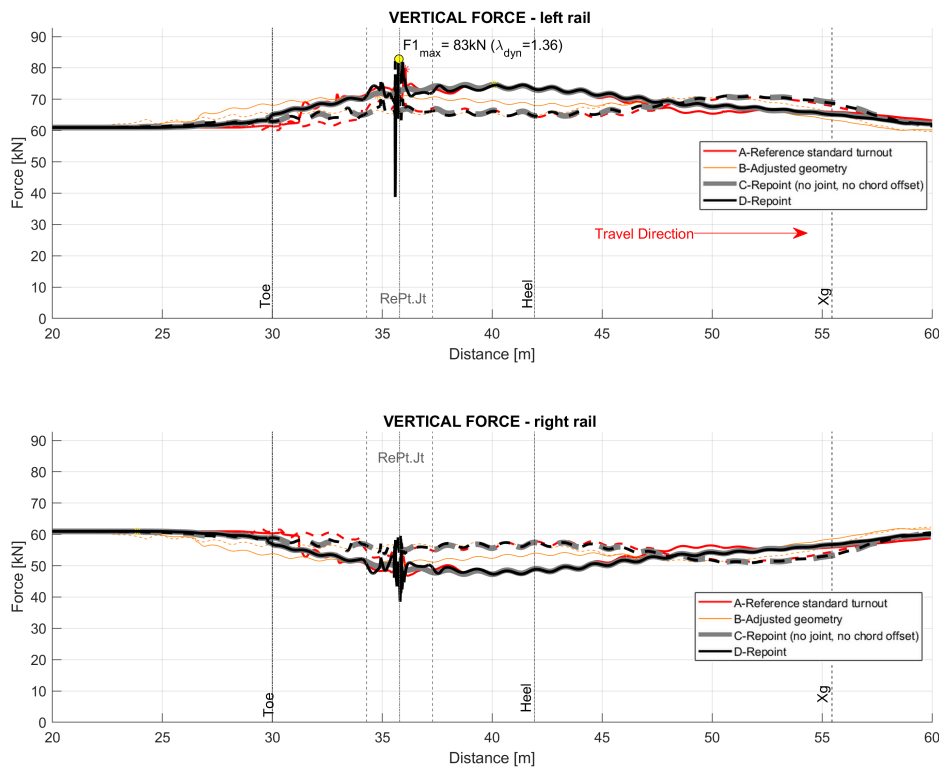
Figure 15.   Vertical forces on outer (top) and inner (bottom) rails. Solid lines (–) for leading axle and dashed lines (- -) for trailing axle.

2.4.   *Diverging direction analysis: Wheel-rail contact pressure*

Figure 16 represents the equivalent Hertzian contact stresses. For CEN56 CV, the highest contact stresses are observed during change of contact from stock to switch rail (between toe and <37m). The high transient nature of the contact conditions, i.e. multiple and sudden contact jumps, leads to very high values (in the order of more than 3GPa, equivalent Hertzian pressure) on the outer rail. This condition may lead to fatigue and deformation of the switch rails at their thinnest and weakest part. On the other hand, the Repoint switch demonstrates a lower value at the start due to the use of inclined rails, and a much smoother transition in the same area, maintaining low contact pressure throughout the switch panel. The reason being a normal crowned rail shape is maintained throughout the switch panel and optimum wheel-rail contact conditions are ensured.

However, there is an exception with the joint, where very high values are seen under the transient load over short distance/duration. Note that towards and beyond the heel, as previously explained, both systems lead to inevitably high quasi-static steering forces in the curved section of the turnout in this very short switch example. Overall, this indicates that the current Repoint design leads to acceptable contact conditions. Nevertheless, tangential contact conditions need to be analysed in more detail to establish the level of wear or rolling contact fatigue to be expected, especially those high instances at the joint.
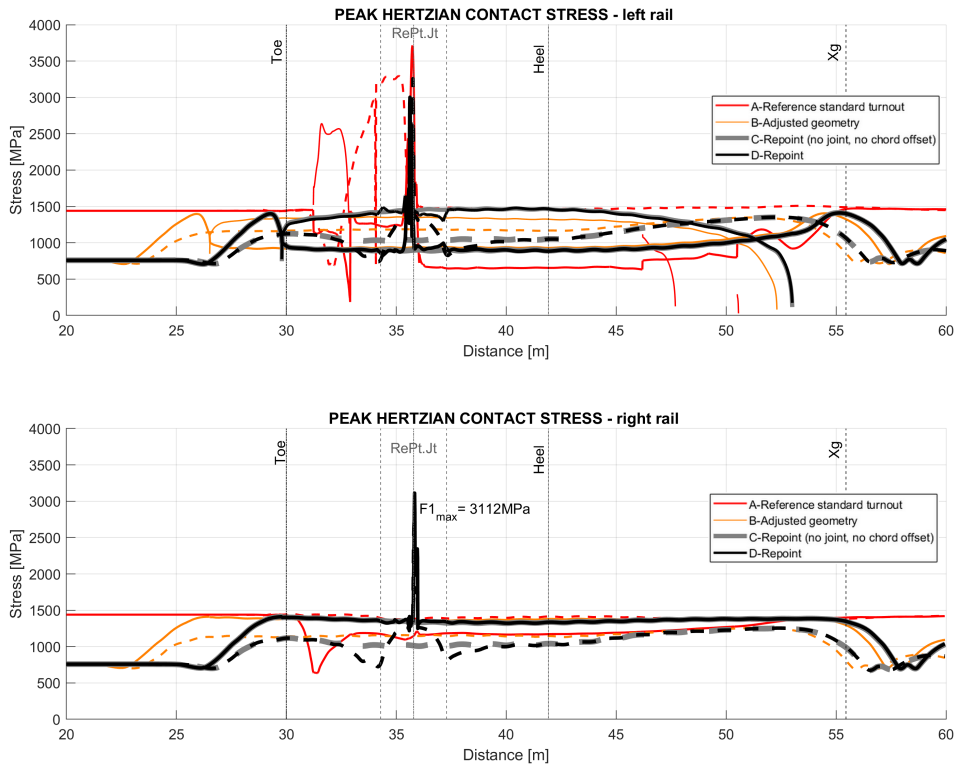
Figure 16. Peak Hertzian contact stress on outer (top) and inner (bottom) rails. Solid lines (–) for leading axle and dashed lines (- -) for trailing axle. Where two lines of the same type co-exist, this indicates multiple contact point.

2.5. *Diverging direction analysis: wear and RCF indicators*

Figure 17 shows the Tγ output indicating the level of energy spent within each contact patch under the action of the creep forces and creepages. The conditions normally associated with rolling contact fatigue (RCF) for a grade 260 rail is highlighted in yellow background colour, between 20 N and 160 N (peak value estimated at 65 N is indicated with a horizontal semi-dashed line) [27]. The white background area above 160 N is entirely dominated by wear. Note the logarithmic y-axis scale on this plot. Where two lines of the same type are present, this indicate double point contact. This is the case for Repoint on the outer rail throughout the curve, and for the CEN56 CV on entry (between 31.2 m and 33 m).

On the outer rail, very high wear is observed due to the leading wheel being in flange contact through the switch curve. On the CEN56 CV, high wear occurs slightly later (after the toe) because initially the axle is not steering until the kink of the switch rail forces it back into the curve; however the contact sustains a much higher wear level, mostly because of the vertical rail installation. In Repoint the onset of wear appears at the toe location at a sustained high level. The passage over the joint and the chord offset also leads to either an increase of Tγ (1st part of chord offset) or a decrease towards RCF region (2nd part of chord offset). The rapid change of contact conditions about the joint centre also generates strong transient effects. Note that both trailing wheels on both designs have a much lower energy output on both outer and inner rails and appear
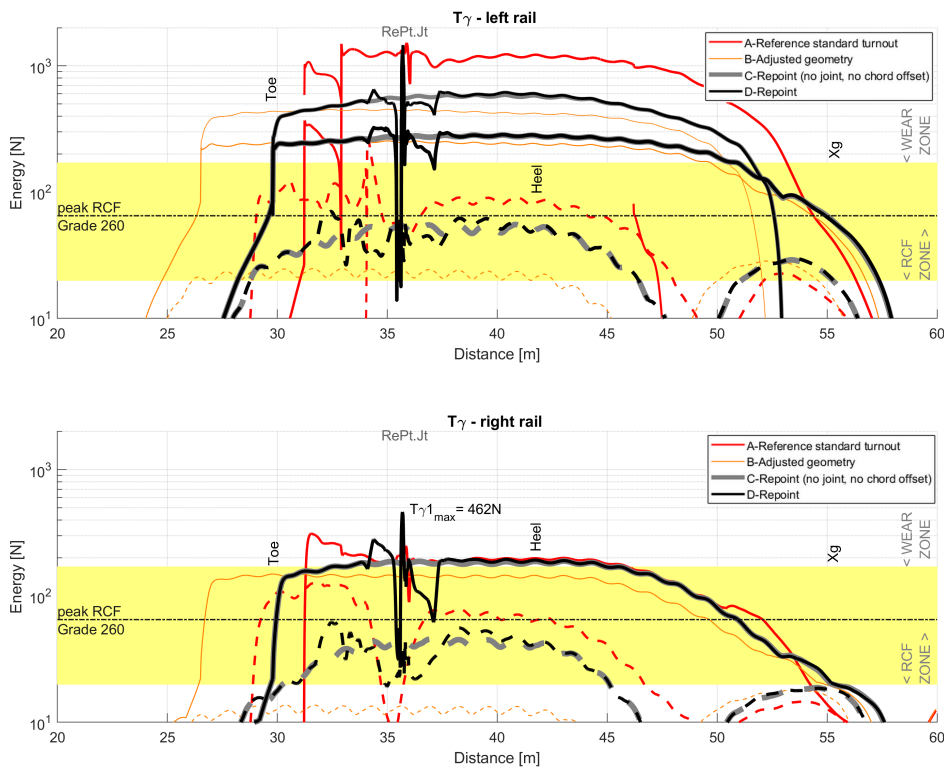
Figure 17.   Tγ energy output, indicating wear (white background) and RCF (yellow background) zones, on outer (top) and inner (bottom) rails. Note the y-axis logarithmic scale. Solid lines (–) for leading axle and dashed lines (- -) for trailing axle. Where two lines of the same type co-exist, this indicates multiple contact point.

to be in a region triggering RCF. The CEN56 CV remains mostly above the peak RCF value, whilst Repoint is generally below. Finally, the Repoint joint in its current form could be expected to suffer high wear on the outer rail and potentially RCF on the inner rail. The next section provides a brief analysis of cumulative wear prediction.

Note that the idealised curve does not produce a significantly different damage regime, apart for the trailing wheelset, which is maintained below the RCF region. This means that under current physical and geometrical constraints (lead length and crossing angle), it is difficult or impossible to avoid wear and RCF degradations for CV type switches. However, if the turnout can be lengthened and the crossing angle made more shallow, there is scope to reduce RCF from the trailing wheelsets.

3.   Diverging direction analysis: initial results of long-term wear

In order to better understand the long-term behaviour of the joint, wear analysis was performed using the VI-Rail wear toolkit [19]. A loop algorithm simulates a mix of traffic in the diverging direction. The traffic mix includes 2 passenger units and 2 locomotives (80% full traction and coasting), as well as 9 loaded freight wagons with a wide range of representative measured worn wheel shapes. Figure 18 presents preliminary results of this study in terms of cumulative wear progression and achieved worn geometry.

On the outer rail the wear can be seen on the crown of the rail and more predominantly
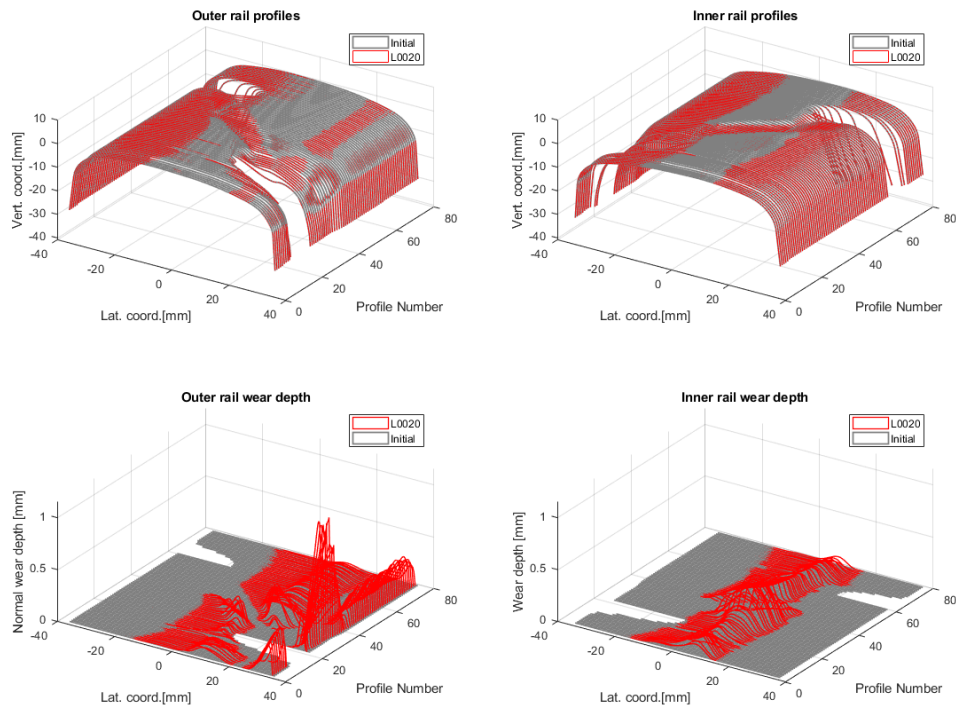
Figure 18.   Wear analysis of Repoint joint on the outer rail and inner rail showing initial and worn profiles (top) as well as calculated wear depth (bottom). Profile ID is in increasing order of appearance (not equidistant).

in the gauge corner. A spike is observed on the inner edge of the fixed part of the joint, after the flange contact leaves the movable part and transfers onto the fixed part with a high dynamic factor. Note that on Figure 18 the profiles are shown plotted against their index rather than track position.

On the inner rail, the cumulated contact conditions are wearing the top crown of the rail as expected with respect to conventional application of expansion joints in straight or large radius curves. Further analyses would be required to investigate the performance of the joint over time, considering a mix of traffic in the through and diverging routes, and to guide with the redesign of the joint to cope with curving wheel-rail contact conditions, while still allowing mechanical locking in several route positions and differential wear on movable and fixed parts.

4.   Conclusions

The benefits of Repoint in terms of wheel-rail contact have been demonstrated on the turn-out direction in the initial part of the switch panel, between the toe and the heel position. Through this tight curving transient section, the curving behaviour of vehicles on conventional switches generally leads to high maintenance requirements of the rail material (high rail wear and RCF) and track geometry (e.g. tamping). For Repoint, this suggest that with the inclined rail design, the constant rail cross section and smooth entrance into the switch curve provides an opportunity to improve the wheel-rail contact conditions, and reduce transient loads and associated rail damage in this early part of the

switch. Beyond the initial transient behaviour of the switch panel, steady state curving conditions are unavoidable on a short switch, irrespective of the switch type.

The concept was also analysed on the through route at speeds up to 200 kph and, despite very short transient loads in the area of the joint, the advantage of removing the conventional stock-switch rail assembly clearly shows benefits in terms of lowering rail damage and improvement of passenger comfort.

Whilst the current version of Repoint already shows different advantages over traditional track switching solutions, it also presents several opportunities for improvement. On both through and diverging routes, the results also show that the detailed design of the Repoint joint is crucial to the success and evolution of this innovation. In particular, it appears that for short switches and tight radius curves, the expected flange contact of the leading wheel with the rail gauge corner is not compatible with the current joint design, inspired from an expansion joint for use on straight track applications. This condition leads to lateral transient loads and local damage mechanisms of the joint: high deformation in load transfer and wear. Differential wear is also likely to occur between the moveable and fixed part of the joint depending on the mix of traffic between through and diverging route(s). Further rail wear analysis is suggested as future work to properly estimate the wear process of corresponding elements of the switch panel and advise on both functional shape and material to be used for the reliable design of the Repoint joint.

Acknowledgements

References

[1] Dow A. The railway: British track since 1804. Pen & Sword Transport Books Ltd; 2014.
[2] Bemment S. Repoint: reduntdantly engineered points for enhanced reliability and capacity of railway track switching. In: 10th World Congress on Railway Research (WCRR); November; Sydney, Australia; 2013.
[3] Bemment S. Redundantly engineered track switching for enhanced railway nodal capacity. In: 1st IFAC ACATTA Workshop; September; Istanbul, Turkey; 2013.
[4] SD Bemment et al. Rethinking rail track switches for fault tolerance and enhanced performance. Journal of the Institution of Mechanical Engineers. 2016;Part F: Rail and Rapid Transit:9.
[5] Operational Failures Modes of Switches and Crossings, Public Deliverable D1.3.1, Capacity4Rail project SCP3-GA-2013-605650, European Commission. 2015.
[6] Lagos RF, Alonso A, Vinolas J, Prez X. Rail vehicle passing through a turnout: analysis of different turnout designs and wheel profiles. Proceedings of the Institution of Mechanical Engineers, Part F: Journal of Rail and Rapid Transit. 2012;226(6):587–602.
[7] Wang P, Xu J, Xie K, Chen R. Numerical simulation of rail profiles evolution in the switch panel of a railway turnout. Wear. 2016;366-367:105 – 115.
[8] Nielsen JC, Pålsson BA, Torstensson PT. Switch panel design based on simulation of accumulated rail damage in a railway turnout. Wear. 2016;366-367:241 – 248; contact Mechanics and Wear of Rail / Wheel Systems, CM2015, August 2015.
[9] Johansson A, Pålsson BA, Ekh M, Nielsen JC, Ander MK, Brouzoulis J, Kassa E. Simulation of wheelrail contact and damage in switches & crossings. Wear. 2011;271(1):472 – 481.

[10] Pålsson BA. Design optimisation of switch rails in railway turnouts. Vehicle System Dynamics. 2013; 51(10):1619–1639.

[11] Nicklisch D, Kassa E, Nielsen J, Ekh M, Iwnicki S. Geometry and stiffness optimization for switches and crossings, and simulation of material degradation. Proceedings of the Institution of Mechanical Engineers, Part F: Journal of Rail and Rapid Transit. 2010;224(4):279–292.

[12] Markine V, Steenbergen M, Shevtsov I. Combatting rcf on switch points by tuning elastic track properties. Wear. 2011;271(1):158 – 167.

[13] Li X, Torstensson P, Nielsen J. Simulation of vertical dynamic vehicletrack interaction in a railway crossing using green's functions. Journal of Sound and Vibration. 2017;410:318 – 329.

[14] Andersson C, Dahlberg T. Wheel/rail impacts at a railway turnout crossing. Proceedings of the Institution of Mechanical Engineers, Part F: Journal of Rail and Rapid Transit. 1998;212(2):123–134.

[15] Bezin Y, Grossoni I, Neves S. Impact of wheel shape on the vertical damage of cast crossing panels in turnouts. In: 24th International Symposium on Dynamics of Vehicles on Roads and Tracks; August; 2015.

[16] Ma Y, Mashal AA, Markine VL. Modelling and experimental validation of dynamic impact in 1:9 railway crossing panel. Tribology International. 2018;118:208 – 226.

[17] Grossoni I, Bezin Y, Neves S. Optimisation of support stiffness at railway crossings. Vehicle System Dynamics. 2017;0(0):1–25.

[18] Okuda H, Asanuma K, N M, Wakui H. Dynamic load, resistance and environmental performance of floating ladder track. Quarterly Report of RTRI (Railway Technical Research Institute) (Japan). 2004 May;45(3):149–155.

[19] VI-grade GmbH, VI-Rail 18.0 Documentation, VI-Rail Wear, www.vi-grade.com. 2017.

[20] Network Rail 2006. Track Design Handbook, NR/SP/TRK/0049 Issue 9. 2006.

[21] Hallade M. Nouvelle méthode de raccordement des courbes. In: Revue Générale des Chemins de Fer; April; 31; 1908.

[22] Hallade handbook / theory and design. LMS Railway; 1946.

[23] GB Patent: Loughborough University. 'Railway Points Operating Apparatus' (GB 2516707). 2013 12.

[24] GB Patent: Loughborough University. 'Railway Points' (GB 2516706). 2013 12.

[25] GB Patent: Loughborough University. 'Railway Track Crossing' (GB2516712). 2013 12.

[26] Bezin Y. Designing future turnouts where research capabilities meet industry needs. In: Rail Tech Expert Series; January 26th; Paris, France; 2016.

[27] Burstow M. Whole life rail model application and development for RSSBcontinued development of an RCF damage parameter. Rail Standards and Safety Board; 2004. Report no.:.

Appendix

This section presents the parameters used in various simulation scenarios under consideration for different studies presented in this article.

Table 1.   Simulation parameters

Vehicle mass properties and inertias

Component	Mass (Mg)	Ixx; Iyy; Izz (Mg.m^2)
Car body	39	55; 1581; 1564
Bogie frame	2.5	1.74; 1.6; 3.2
Wheelset	1.4	0.87; 0.166; 0.87
Axle box	0.02	-

Vehicle dimensions

Component	Spacing (m)
Bogie centre	16
Axle	2.6

Track model properties

Component	Mass (kg)	Ixx (kg.m^2)
Rail	60	10
Sleeper/ballast	500	100

Track model stiffness and damping

Property	Vertical (z)	Lateral (y)	Roll (θ)
Rail pad stiffness (MN/m or /rad)	50	43	10
Rail pad damping (kNs/m or /rad)	200	240	10
Ballast support stiffness (MN/m or /rad) per sleeper	1000	37	10
Ballast support damping (kNs/m or /rad) per sleeper	1000	240	10

Vehicle suspension properties

Property	Vertical (z)	Lateral (y)	Yaw (Ψ)
Secondary airspring stiffness (kN/m or /rad) per bogie*	216	188	174
Secondary airspring damping (kNs/m or /rad) per bogie*	13.2	11.5	12.2
Secondary yaw dampers (kNs/m) per bogie	-	-	220
Secondary lateral damper (kNs/m) per bogie	-	38	-
Primary stiffness (kN/m or /rad) per wheelset	1800	22000	12000
primary damping (kNs/m or /rad) per wheelset	16	18	-

*Per side.